

Central Lancashire Online Knowledge (CLoK)

Title	Mechanical characterisation of the lateral collateral ligament complex of the ankle at realistic sprain-like strain rates
Type	Article
URL	https://clock.uclan.ac.uk/30326/
DOI	https://doi.org/10.1016/j.jmbbm.2019.103473
Date	2020
Citation	Rochelle, David Christopher, Herbert, Anthony, Ktistakis, Ioannis, Redmond, Anthony Charles, Chapman, Graham and Brockett, Claire Louise (2020) Mechanical characterisation of the lateral collateral ligament complex of the ankle at realistic sprain-like strain rates. <i>Journal of the Mechanical Behavior of Biomedical Materials</i> , 102. p. 103473. ISSN 1751-6161
Creators	Rochelle, David Christopher, Herbert, Anthony, Ktistakis, Ioannis, Redmond, Anthony Charles, Chapman, Graham and Brockett, Claire Louise

It is advisable to refer to the publisher's version if you intend to cite from the work.
<https://doi.org/10.1016/j.jmbbm.2019.103473>

For information about Research at UCLan please go to <http://www.uclan.ac.uk/research/>

All outputs in CLoK are protected by Intellectual Property Rights law, including Copyright law. Copyright, IPR and Moral Rights for the works on this site are retained by the individual authors and/or other copyright owners. Terms and conditions for use of this material are defined in the <http://clock.uclan.ac.uk/policies/>

Mechanical characterisation of the lateral collateral ligament complex of the ankle at realistic sprain-like strain rates

1 Abstract

2 BACKGROUND

**3 Synthetic interventions continue to evolve with the progression made in materials
4 science, surgical technologies and surgical methods. To facilitate the evolution of
5 synthetic devices for lateral ankle repair a better understanding of the mechanical
6 properties and failure mechanisms of the lateral collateral ligament (LCL) complex
7 is required. This study aimed to improve understanding of the mechanical
8 properties and failure modes of the LCL complex at strain rates representative of
9 sprain.**

10 METHOD

**11 The LCLs were dissected from six human cadavers to produce individual bone-
12 ligament-bone specimens. A mechanical testing device uni-axially loaded the
13 ligaments in tension. Initially, preconditioning between two Newtons and a load
14 value corresponding to 3.5 % strain was conducted for 15 cycles, before extension
15 to failure at strain rate of 100 %. s^{-1} . The results were stratified by age, weight and
16 body mass index (BMI) to explore potential correlations with ligament ultimate
17 failure load or ligament stiffness.**

18 RESULTS

ATFL – Anterior Talofibular Ligament
CFL – Calcaneofibular Ligament
LCL – Lateral Collateral Ligament
PTFL – Posterior Talofibular Ligament

19 **The mean ultimate failure loads and the 95 % confidence intervals for the ATFL,**
20 **calcaneofibular (CFL) and posterior talofibular (PTFL) ligaments were 263.6 ± 164.3**
21 **N, 367.8 ± 79.8 N and 351.4 ± 110.8 N, respectively. A strong positive Pearson**
22 **correlation was found between BMI and ultimate failure load of the CFL ($r = .919$; P**
23 **= .01). A non-significant relationship was found between the mechanical properties**
24 **and both age and weight. The ATFL avulsed from the fibula four times, the CFL**
25 **avulsed from the fibula twice, the PTFL avulsed from the talus twice and all**
26 **remaining failures were mid-substance.**

27 **CONCLUSION**

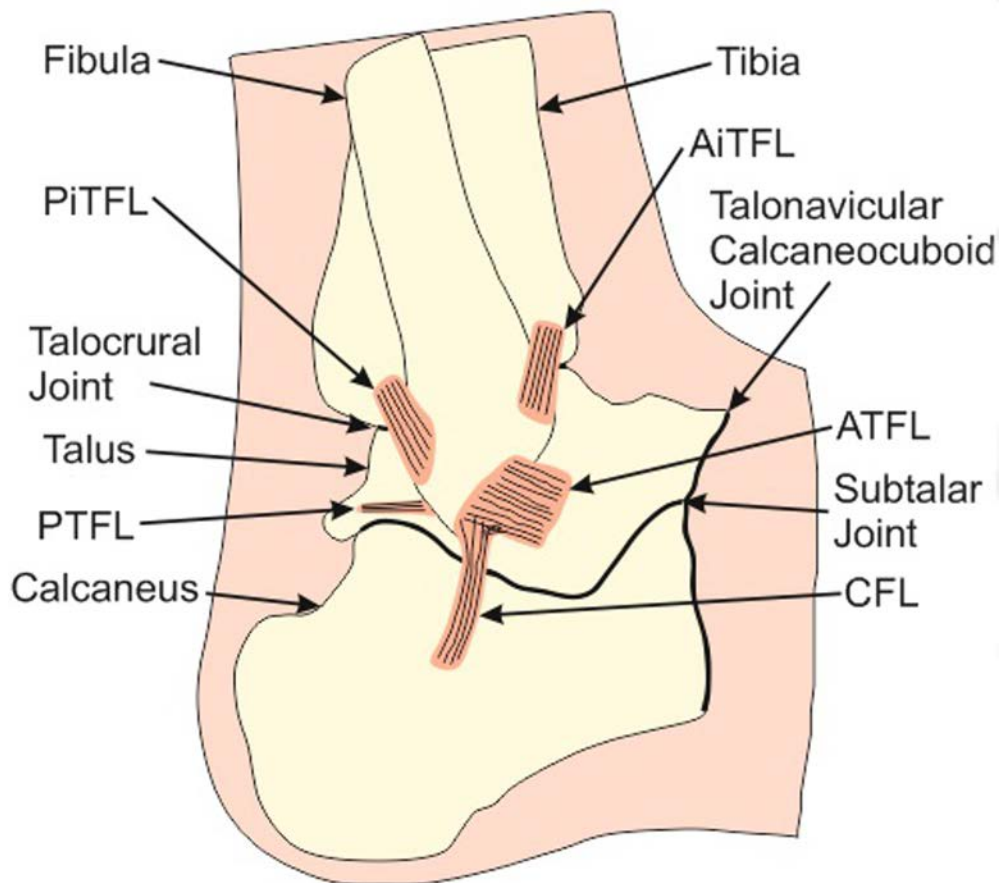
28 **The results identify the forces required to induce failure of the individual ligaments**
29 **of the LCL complex and the related failure modes of individual ligaments. A**
30 **correlation may exist between BMI and the ultimate failure load of the CFL and**
31 **PTFL, although a greater sample size is required for confirmation.**

32 **Keywords**

33 Characterisation; Ankle; Ligament; Sprain

34 **Introduction**

35 The lateral collateral ligament (LCL) complex of the ankle (see Figure 1), consists of
36 the anterior talofibular ligament (ATFL), calcaneofibular ligament (CFL) and posterior
37 talofibular ligament (PTFL). The LCLs of the ankle are collectively responsible for the
38 stabilisation of the talocrural joint on the lateral side and the CFL also plays a role in
39 the stabilisation of the subtalar joint.



40

41 **Figure 1.** Lateral view of the ankle highlighting the LCL complex (ATFL, CFL & PTFL), the syndesmosis
 42 (AiTFL & PiTFL), the talocrural joint, the subtalar joint, the talonavicular calcaneocuboid joint and the
 43 bones of the ankle (fibula, tibia, talus and calcaneus).

44 The ATFL is the most frequently injured LCL in a typical lateral ankle sprain, followed
 45 by the CFL and finally the PTFL.^{3,16} In cases of severe sprain or in people, such as elite
 46 athletes, wherein whom restoration of stability is important, surgical stabilisation
 47 may be performed. The current preferred standard is the Broström-Gould procedure
 48 in which ruptured ligaments are stabilised with sutures. If this approach is
 49 inadequate or has failed or if the patient has an increased BMI, general ligament
 50 laxity or is a high-demand athlete, then stabilisation with synthetic ligaments may be
 51 attempted.¹

52 Natural ligaments exhibit a viscoelastic response to strain, starting with a
 53 progressively stiffer nonlinear toe region followed by a linear loading region. The
 54 response of ligamentous tissue is believed to be strain rate dependent due to the

55 inherent viscoelastic nature of the tissue.⁶ This viscoelasticity causes ligaments to
56 display hysteresis, due to the fluid component of the ligament being redistributed
57 and balanced by the stress carried by the solid component of the ligament. When
58 the lateral collateral ligament of the knee was tested at strain rates greater than 100
59 $\% \cdot s^{-1}$, a strain rate representative of inducing sprain in real-world events, it was
60 found that the strain-rate dependency of the ligament can be neglected as there is
61 insufficient time for appreciable ligament relaxation.⁶ The ligaments of the ankle
62 have been reported to be generally insensitive to strain rate.⁹ Conversely, the
63 mechanical properties of the LCLs have been reported to be significantly affected by
64 strain rates both above and below 100 $\% \cdot s^{-1}$.³

65 Research articles detailing the mechanical characteristics of the LCL complex are
66 scarce.^{3,9,16,17} None of the previous papers report mechanical characteristics of the
67 LCL complex tested at realistic sprain-like strain rates. Attarian et al. (1985) and Funk
68 et al. (2000) characterised the LCL complex at strain rates considerably higher than
69 those which occur during a sprain event.^{3,9} Although ligaments are considered
70 relatively insensitive to strain rates over 100 $\% \cdot s^{-1}$ the effect on the failure mode of
71 the ligaments is not understood. The absence of literature on this topic is potentially
72 due to the difficulty faced when gripping ankle ligament tissue, as previously
73 reported.¹⁶ A lack of published work in this area has hindered the understanding of
74 the mechanical requirements and failure modes of synthetic interventions for lateral
75 ankle sprain.

76 This study aimed to improve understanding of the mechanical properties and failure
77 modes of the LCL complex at strain rates representative of real-world sprain events.

78 **Materials and Methods**

79 **2.1 Samples**

80 Six fresh frozen human cadaveric feet, sourced from MedCure (USA), were used in
 81 the study. Ethical approval was granted by the University of Leeds Research Ethics
 82 Committee (MEEC 15-020). Exclusion criteria for the tissues included a reported
 83 prior lower limb trauma or surgery, or a history of diabetes. The mean (\pm 95 %
 84 confidence intervals) donor age was 56.2 ± 12.2 years, BMI was 22.3 ± 2.9 kg.m⁻²
 85 (normal) and there were three males and three females. A summary of donor
 86 information is shown in Table 1.

87 **Table 1.** Tissue donor demographic details. The mean and 95 % confidence interval (CI) is given for
 88 age, weight and body mass index (BMI). (M – male, F – female, A.A – African American, C – Caucasian,
 89 R – right & L – left).

Sample	Age (years)	Sex	Race	Weight (kg)	BMI (kg.m ⁻²)	L/R Foot
1	72	M	A.A	71	22.4	R
2	60	F	C	53	18.9	L
3	49	F	C	49	20.9	R
4	61	M	C	66	21.4	R
5	38	M	C	85	27.0	L
6	57	F	C	61	23.2	R
Mean	56.2	-	-	64.1	22.3	-
\pm CI	± 12.2	-	-	± 13.8	± 2.9	-

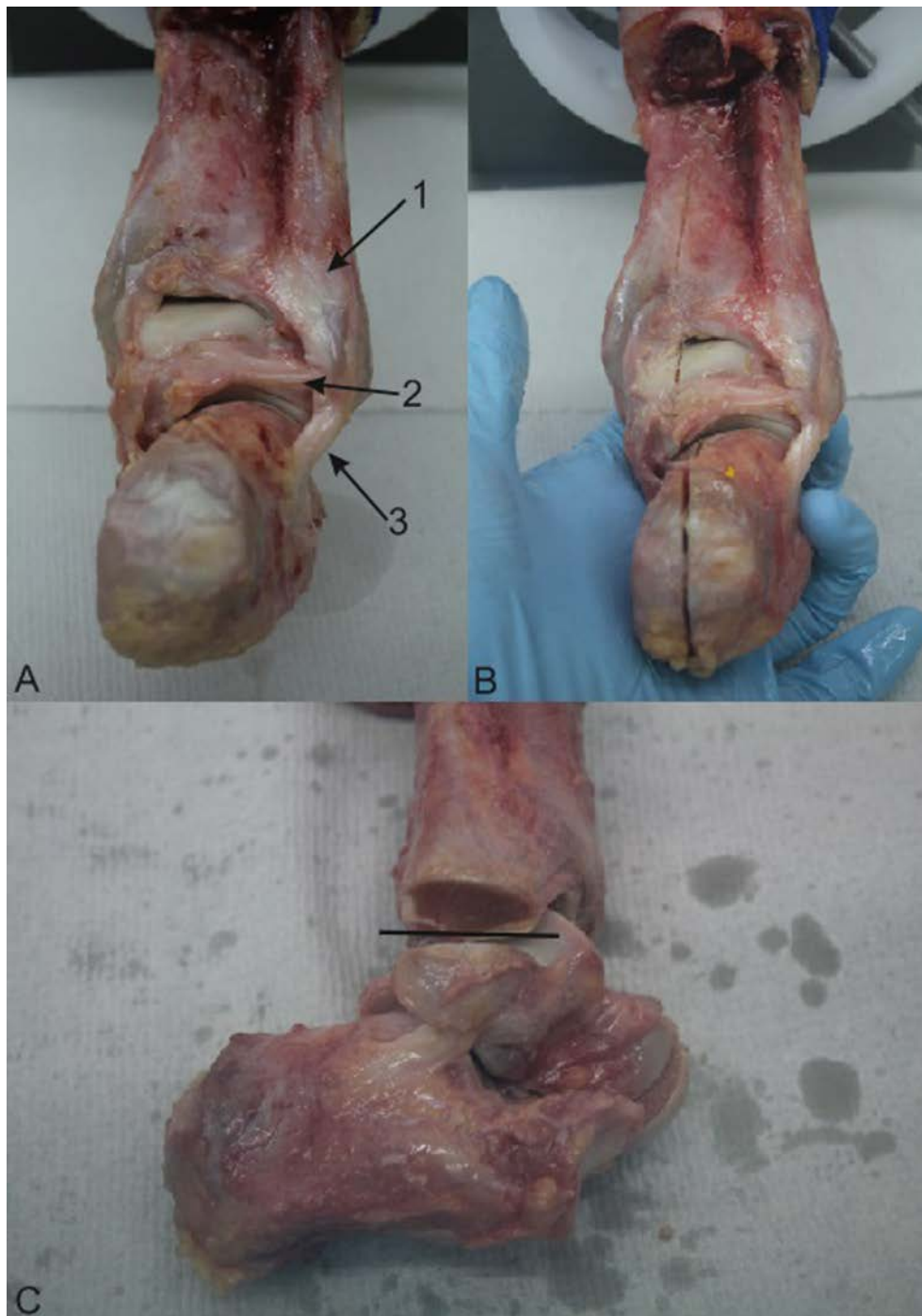
90

91 **2.2 Sample Preparation**

92 The feet were stored in a -80 °C freezer, compliant with the Human Tissue Act, until
 93 they were tested. Samples were thawed for 48 hours at 4 °C in a refrigerator prior to
 94 dissection. After at least 24 hours of thawing, each foot was imaged, at a resolution
 95 of 82 μ m, using a SCANCO Medical xtreme CT scanner (SCANCO Medical, Brüttisellen,
 96 Switzerland). Each scan lasted approximately 90 minutes and was performed to
 97 ensure no major undiagnosed damage was present.

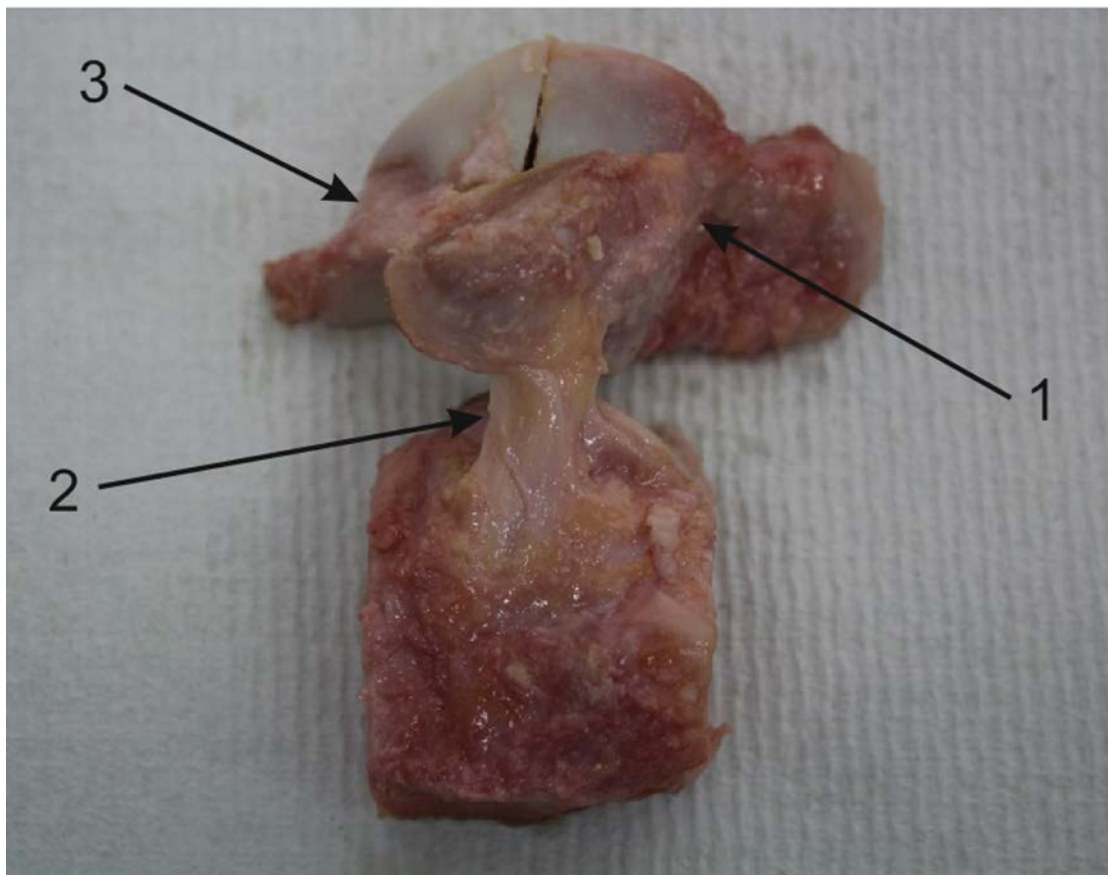
98 The LCL complex was dissected intact from each foot while preserving the
 99 syndesmosis joint for future study, as shown in Figures 2 & 3. Firstly, all fascia and

100 soft tissue were dissected from around the ankle by a foot and ankle specialist
101 consultant orthopaedic surgeon. Next, the forefoot was removed by transecting
102 along the talonavicular calcaneocuboid joint. Using an oscillating bone saw, a sagittal
103 cut was made through the entirety of the calcaneus and talus, as shown in Figure 2,
104 Panel B. The lateral ankle complex was then removed by a transverse cut through
105 the fibula, separating the LCL complex from the syndesmosis, as shown in Figure 2,
106 Panel C. The cut was made from in-between the attachment points of the ATFL and
107 anterior inferior talofibular ligament (AiTFL) to in-between the attachment points of
108 the PTFL and posterior inferior talofibular ligament (PiTFL). The talus was then split in
109 half with a coronal cut creating an anterior and posterior bone attachment segment
110 for the ATFL and PTFL, respectively. Finally, the calcaneus was reduced in size and
111 shaped to fit within the gripping fixture by performing two parallel coronal cuts
112 either side of the attachment point and one transverse cut distally to the attachment
113 point, as shown in Figure 3. The tissue hydration level of the ankle complex was
114 maintained by wrapping the complex in phosphate-buffered saline (PBS) soaked
115 paper towel.¹¹



116

117 **Figure 2.** The dissection protocol employed to remove the LCL complex from the rearfoot. **A** illustrates
118 the intact rearfoot and provides a clear view of the PiTFL (1), PTFL (2) and CFL (3). **B** illustrates the
119 sagittal cut made to separate the medial and lateral aspects of the rearfoot. **C** illustrates the
120 transverse cut (black line) made through the fibula to separate the LCL complex and syndesmosis.



121

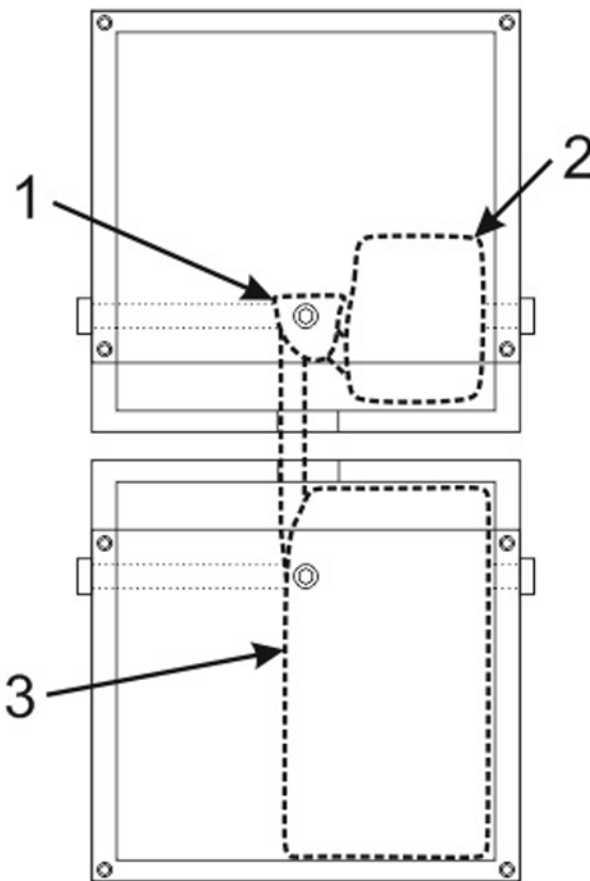
122 **Figure 3.** The LCL complex fully dissected prior to testing. The coronal cut into talus has been
123 performed, creating separate bone pieces for the ATFL and PTFL, and the calcaneus has been shaped
124 to fit within the bespoke testing grip. The ATFL (1), CFL (2) and PTFL (3) are shown.

125 Post-dissection ligament lengths were measured using Vernier callipers with the
126 ligaments orientated in line with their collagen fibres and the slack in the ligament
127 was removed by hand. The ligaments were measured once, from the centre of one
128 insertion to the centre of the other.

129 **2.3 Testing Protocol**

130 Each ligament of the LCL complex was tested individually whilst the complex was
131 kept intact. The CFL was characterised first, then the ATFL followed by the PTFL.
132 Tissue rehydration was performed to ensure the viscoelastic nature of ligaments
133 could act efficiently during the testing. Immediately before the characterisation of
134 the CFL, the complex was submerged in PBS for 30 minutes. The complex was then
135 submerged for 15 minutes prior to testing the ATFL and a further 15 minutes prior to

136 testing the PTFL due to the short length of time taken for each test. Testing the
137 individual ligaments as an intact complex was facilitated by a bespoke gripping
138 fixture. The bone segments at each end of the ligaments were fixed within the
139 gripping fixture using six gripping bolts for each bone attachment segment ensuring
140 collagen fibre alignment, as shown in Figure 4.



141

142 **Figure 4.** The LCL complex fixed into the bespoke gripping fixture with the CFL prepared for
143 characterisation. The ATFL and PTFL, and their bony attachments from the fibula (1) to the talus (2)
144 are within the top pot and the calcaneus (3) is within the bottom pot.

145 The mechanical characterisation was performed using an Instron ElectroPuls E10000,
146 with a 1 kN load cell (Instron, Buckinghamshire, UK). A floating joint was used to
147 attach the top grip to the Instron to correct for any unintended malalignment within
148 the setup.

149 Preconditioning was completed to ensure specimens were in an appropriate
150 physiological state of readiness prior to failure testing and fluid redistribution had

151 occurred within the specimens.¹⁴ Fifteen cycles of preconditioning following a
152 sinusoidal waveform, ranging between two Newtons and a load value corresponding
153 to 3.5 % strain, were performed at a frequency of 0.83 Hz. The 3.5 % strain value
154 represents the minimum amount of strain accumulated by any of the LCLs during
155 one step of a normal walking cycle (10 degrees dorsiflexion through to 20 degrees
156 plantarflexion).⁷ The preconditioning load values representing 3.5 % strain were
157 determined in a preliminary test of each ligament tested under strain control at a
158 rate of 10 %·s⁻¹. The frequency of 0.83 Hz is equivalent to the rate of normal walking
159 (approximately one full gait cycle per second).

160 Following preconditioning, the specimens were then ramp loaded to failure at a
161 strain rate of 100 %·s⁻¹. A strain rate of 100 %·s⁻¹ was selected to be representative of
162 sprain, having previously been suggested to be a suitable injury strain rate for
163 anterior cruciate ligament injury.⁴ The following equation, incorporating real-world
164 inputs, also suggests that a strain rate of 100 %·s⁻¹ is appropriate to replicate ankle
165 ligament sprain.

166
$$\dot{\epsilon} = \frac{\Delta L}{Lt}$$

167 Where $\dot{\epsilon}$ is the strain rate, ΔL is the change in length of the ATFL from neutral
168 position to maximum plantarflexion (4.5 mm),² L is the length of the ATFL in the
169 neutral position (16.3 mm)² and t is the time taken for the sprain motion of an ankle
170 (0.3 s).⁸

171 **2.4 Data Analysis**

172 The mode of failure was determined via physical and visual examination of the
173 specimens. Any specimens where the ligament had torn away from bone, torn
174 cartilage away from bone or torn a small fragment of bone away from bone were
175 categorised as an avulsion. Any intra-ligamentous failures were defined as mid-

176 substance failures. After the experimental testing, post-processing was completed to
177 calculate the ultimate failure load and stiffness of each ligament from each donor.
178 The linear stiffness value (k_1) was calculated using a custom Matlab algorithm.¹¹
179 Mean values and 95 % confidence intervals for the ligament ultimate failure load,
180 stiffness and length, as well as the donor BMI, weight and age were calculated for
181 the ATFL, CFL and PTFL. A repeated measures ANOVA with a Greenhouse-Geisser
182 correction ($p < .01$) was performed to calculate any significant differences in ultimate
183 failure load or stiffness between the ATFL, CFL and PTFL. Analysis of the data
184 stratified by age, weight and BMI was performed to identify any potential
185 correlations with these patient-specific factors and both ultimate failure load and
186 stiffness. Correlations were calculated for the ATFL, CFL and PTFL individually using a
187 two-tailed Pearson correlation test ($p < .01$).

188 **Results**

189 The post-dissection ligament lengths used to calculate the ligament specific
190 preconditioning limits are provided in Table 2. The CFL was the longest of the three
191 ligaments forming the LCL complex, with mean (\pm 95 % CI) length of 20.0 ± 1.9 mm.
192 The PTFL and ATFL followed in order but were similar in length with mean lengths of
193 13.4 ± 3.2 mm and 12.6 ± 0.9 mm, respectively.

194 **Table 2.** Ligament lengths (mm) for each individual ligament and the mean ligament length and 95 %
195 confidence intervals (CI) for ATFL, CFL and PTFL.

196

197

Sample	ATFL	CFL	PTFL
1	11.62	17.60	10.50

2	11.76	20.66	14.66
3	12.90	19.24	10.54
4	13.50	23.00	18.34
5	12.08	20.06	14.80
6	13.54	19.66	11.66
Mean ± CI	12.6 ± 0.9	20.0 ± 1.9	13.4 ± 3.2

198

199 The mechanical characterisation results for the ATFL, CFL and PTFL are shown in
 200 Table 3. The CFL had the highest mean ultimate failure load ($\pm 95\%$ CI) of $367.8 \pm$
 201 79.8 N followed by the PTFL 351.4 ± 110.8 N, while the ATFL was the weakest $263.6 \pm$
 202 164.3 N. No significant differences were found for the ultimate failure load ($p = .24$)
 203 or stiffness ($p = .30$) between the ATFL, CFL and PTFL.

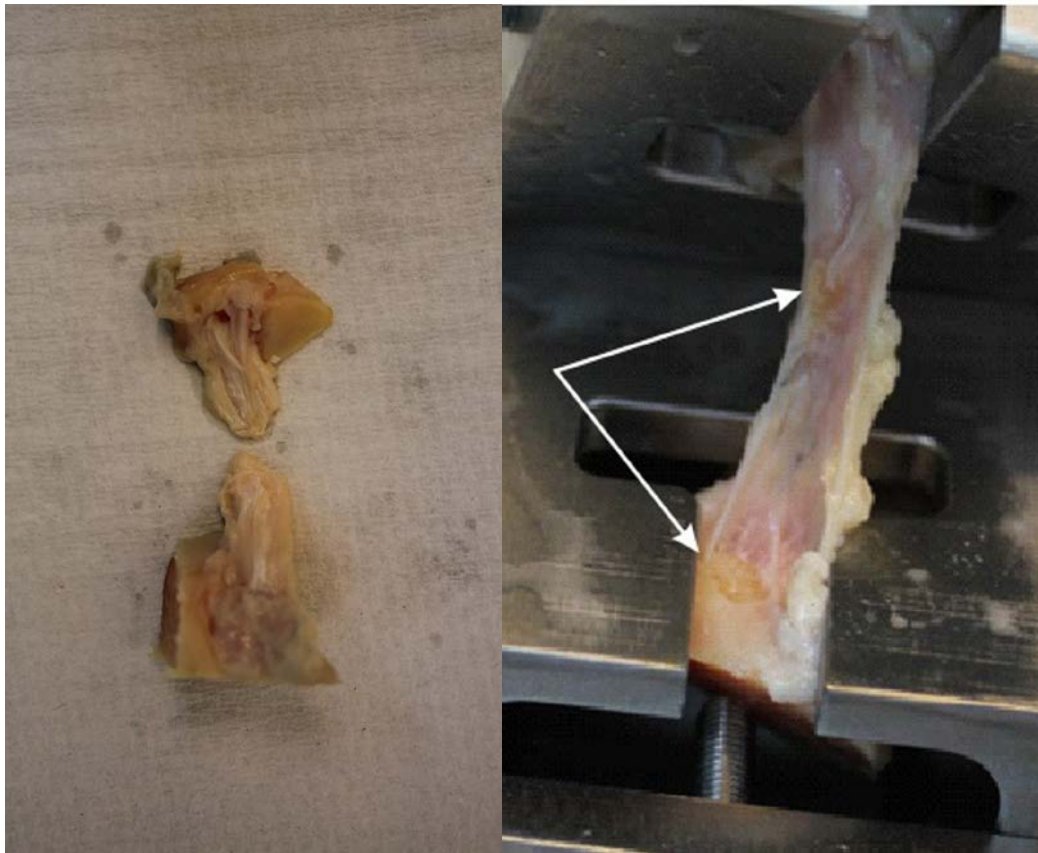
204 **Table 3.** The mean and 95 % confidence intervals (CI) for the ultimate failure load and stiffness results
 205 of the ATFL, CFL and PTFL. As well as the failure mode (A – avulsion and M – mid-substance) and
 206 avulsion location.

	ATFL	CFL	PTFL
Mean			
Ultimate Failure Load	263.6 ± 164.3	367.8 ± 79.8	351.4 ± 110.8
± CI (N)			
Mean Stiffness ± CI (N/mm)	44.7 ± 16.6	45.8 ± 19.0	59.0 ± 10.7
Failure Mode (A/M)	4/2	2/4	2/4
Avulsion Site	Fibula	Fibula	Talus

207

208 The ratio of avulsions to mid-substance failures was similar for the ligament types
 209 tested, as detailed in Table 3. The ATFL avulsed from the fibula in four of the six
 210 tests, the CFL avulsed from the fibula in two of the six tests and the PTFL avulsed
 211 from the talus in two of the six tests. No systematic differences in ultimate failure
 212 load or stiffness were identified between the different failure modes. When avulsion

213 did occur, the site of avulsion was consistent amongst ligament types (see Table 3).
214 Figures 5A and 5B illustrate clear examples of a mid-substance failure and avulsion,
215 respectively.



216

217 **Figure 5. A)** A mid-substance failure where intra-ligamentous failure has occurred. **B)** An avulsion
218 failure where a fragment of bone has also been avulsed from the bone surface (white arrows).

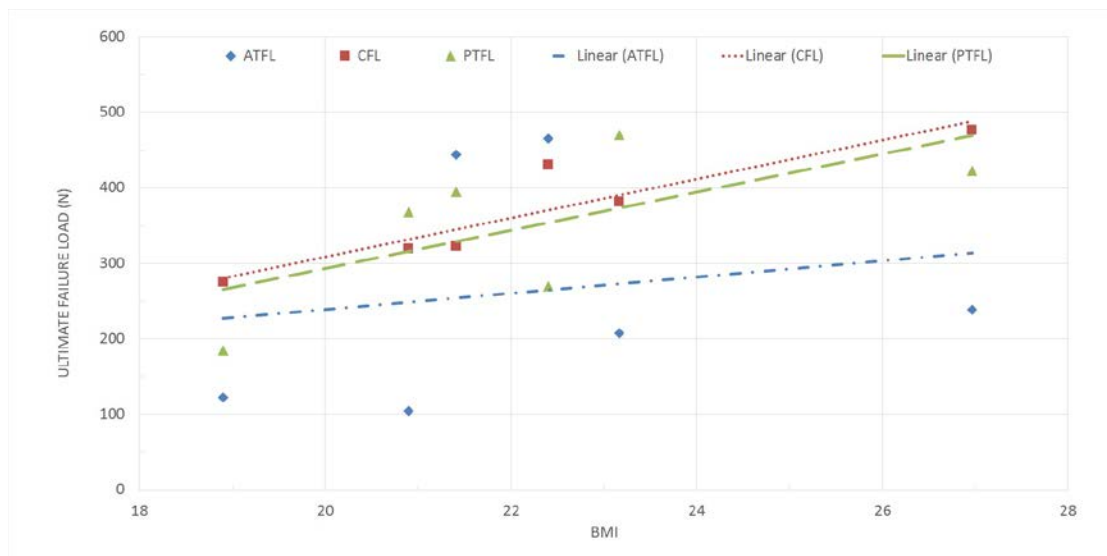
219 The correlation results for the ultimate failure load and stiffness to the patient-
220 specific factors: BMI, weight and age are presented in Table 4. The ultimate failure
221 load of the CFL was found to have a significant strong positive Pearson correlation
222 with BMI ($r = .92$; $p = .01$). The ultimate failure load of the ATFL and PTFL had non-
223 significant Pearson correlation scores ($r = .18$; $p = .73$ and $r = .65$; $p = .16$,
224 respectively). A non-significant relationship was found for both age and weight with
225 relation to both the ultimate failure load and stiffness of the ATFL, CFL and PTFL. Any
226 relationship identified between BMI and stiffness of the ATFL ($r = -.05$; $p = .92$), CFL (r
227 $= .22$; $p = .68$) and PTFL ($r = -.01$; $p = .98$) was also negligible.

228 **Table 4.** The correlation (r-value) and respective significance (p-value) of both ligament ultimate
 229 failure load and ligament stiffness against the patient-specific factors (PSF): BMI, weight and age.

Ligament Property		PSF	r-value	p-value
Failure Load	ATFL	BMI	.184	.727
	CFL	BMI	.919*	.010
	PTFL	BMI	.650	.162
	ATFL	Weight	.516	.395
	CFL	Weight	.874	.023
	PTFL	Weight	.327	.527
	ATFL	Age	.560	.248
	CFL	Age	-.273	.600
	PTFL	Age	-.496	.317
Stiffness (k1)	ATFL	BMI	-.052	.922
	CFL	BMI	.216	.681
	PTFL	BMI	-.013	.981
	ATFL	Weight	.176	.738
	CFL	Weight	.410	.419
	PTFL	Weight	.000	.999
	ATFL	Age	.750	.086
	CFL	Age	-.397	.436
	PTFL	Age	-.340	.510

230 *i indicates result is significant at the .01 level (two-tailed).

231 The ultimate failure load results of the ATFL, CFL and PTFL are plotted against BMI in
 232 Figure 6 with the results for all three ligaments of each donor aligned vertically
 233 according to the donor's BMI. There is no evidence of a systematic tendency for the
 234 ultimate failure load to vary by ligament type either within or between donors.



235
 236 **Figure 6.** A graphical representation of the relationship between BMI and ultimate failure load. The
 237 three ligaments of each donor are vertically aligned according to the BMI of the donor. The ATFL is
 238 shown by blue diamond markers, the CFL by red square markers and the PTFL by green triangle

239 markers. Trend lines are shown for the ATFL (blue dash dot), CFL (red dotted) and PTFL (green
240 dashed).

241 **Discussion**

242 The aim of this study was to improve understanding of the mechanical properties
243 and failure modes of the LCL complex when strained at a rate representative of ankle
244 sprain events in real-life. The mechanical characteristics of the entire LCL complex
245 when loaded at a realistic sprain-like strain rate ($100 \text{ \%} \cdot \text{s}^{-1}$) are reported. The mean
246 ultimate failure load results concur with previously published work, that the CFL and
247 PTFL provide similar levels of support under load and that the ATFL is the
248 weakest.^{3,16} There is however, a large amount variability between specimens, as
249 shown in Figure 6, and there was no clear pattern for which ligament is the strongest
250 or weakest at an individual donor level. Whilst St Pierre et al. (1983) only reports
251 tensile strength of the ATFL they do so, in most cases, for each foot of each
252 individual donor highlighting the substantial variability in ATFL failure load, ranging
253 from 44 N to 556 N. Notably, the ATFL, which is widely established as the weakest
254 LCL, was the strongest for two donors in this study, contradicting the general
255 consensus.^{3,16} The widely established view that the ATFL is the weakest of the LCLs
256 could therefore be incorrect for some people. The cause of this finding is likely
257 multifactorial and a much larger sample size and in-depth patient information is
258 required to substantiate any hypothesis.

259 Stiffness results in this study are similar to those previously reported by Attarian et
260 al. (1985) who strained the LCLs at strain rates considerably higher than $100 \text{ \%} \cdot \text{s}^{-1}$.

261 This paper therefore supports the theory that the strain-rate dependency of
262 ligaments can be neglected when tested at strain rates greater than $100 \text{ \%} \cdot \text{s}^{-1}$.^{6,9} The
263 current findings indicate a range of indicative ultimate failure loading requirements
264 that can further inform the mechanical property specifications for synthetic ankle

265 ligaments. Through improved matching of the mechanical properties, particularly the
266 stiffness, of synthetic ligaments to their natural counterparts joint mobility and
267 stability have the potential to also improve.

268 Both mid-substance failure and avulsion are abundantly prevalent as failure modes
269 of the LCLs. Categorisation of the failure mode is somewhat subjective due to the
270 fibrous nature of ligamentous failure, the difficulty faced differentiating between
271 failure modes and the lack of a standardised definition of avulsion. The location of
272 ligament avulsion was consistent, at the fibula for the ATFL and CFL and at the talus
273 for the PTFL. Siegler et al. (1988) found the AFTL to avulse 58 % of the time and the
274 CFL and PTFL to avulse in 70 % of tests, with remaining specimen failing mid-
275 substance.¹⁶ Attarian et al. (1985) reported eight mid-substance failures and four
276 talar avulsions for the ATFL, eight mid-substance failures, four calcaneal avulsions
277 and four fibula avulsions for the CFL and four mid-substance failures for the PTFL.³ St
278 Pierre et al. (1983) reported 18 talar avulsions, 16 mid-substance failures and two
279 unknown failures.¹⁷

280 The location of ATFL avulsion in this study is inconsistent with those previously
281 reported and an explanation as to why is unclear. Possible explanations include the
282 status of the fibula, the orientation of the ligament or the vastly different strain
283 rates. The fibula was intact for testing in the studies by St Pierre et al. (1983) and
284 Attarian et al. (1985) whereas in this study the fibula was split reducing the amount
285 of bone to be gripped. The orientation of the specimen may differ slightly between
286 this study and the two studies highlighted due to the fibula not being intact,
287 although all studies attempted tensile testing with fibre alignment. The prevalence
288 of avulsion and mid-substance failures are however comparable. The high
289 prevalence of avulsions could be due to the significantly higher local strain proximal
290 to the attachment site of ligaments compared to the central region.¹⁸ The failure

291 mechanism of a ligament is an important consideration prior to a ligament repair
292 being performed as the fixation method may differ depending on whether the
293 ligament needs reattaching to bone or to ligament.

294 A potentially noteworthy finding was the positive correlation between BMI and
295 ultimate failure load values for the ligaments of the LCL complex, specifically the CFL.
296 This finding, from a sample size of six, suggests that the CFL of individuals with a
297 higher BMI have a greater load bearing capacity than those with a lower BMI. This is
298 most likely due to the adaptive remodelling nature of ligamentous structures, as
299 individuals with a greater BMI are likely to apply more stress to the ligament,
300 increasing strength over time.⁵ The BMI of an individual could therefore be an
301 important factor when selecting the appropriate material properties of a synthetic
302 intervention, and notably people with a high BMI who are more often candidates for
303 a synthetic ligament replacement.¹ Therefore, the load bearing capacity of the
304 synthetic, and their fixation devices, should match the mean ultimate failure load to
305 ensure the synthetic does not subsequently fail. The stiffness of the synthetic
306 material, along with the tension applied upon insertion, is arguably more important.
307 A stiffness that is too high could reduce the joint mobility and too low could affect
308 the stability of the joint. Therefore it could be recommended that the stiffness of the
309 synthetic material is also matched to that of the natural tissue results reported.

310 The anatomy of ligaments is often depicted incorrectly in illustrations because of
311 stylistic licence. The previously published pictorial essay does however provide
312 detailed images of the ankle ligament anatomy.¹⁰ Figure 3 shows the attachment
313 points of the ATFL and CFL to the fibula. These attachments are often illustrated as
314 separate insertion points however as shown in Figure 3, the two ligaments
315 commonly attach at the same insertion point on the fibula. It is suggested that the
316 inferior aspect of the ATFL and CFL are connected by arciform fibres,¹⁵ thus forming

317 the lateral fibulotalocalcaneal complex.¹² This observation was also made when
318 performing the dissections for this study. The results of this study however suggest
319 that the connecting fibres are not of a sufficient strength to cause both the ATFL and
320 CFL to rupture simultaneously. The CFL was tested first in every instance and the
321 results of the ATFL are still similar to those previously published, where they were
322 tested without the arciform fibres present.¹⁶

323 The limitations to the study predominantly centre on the use of human cadaveric
324 tissue. The main limitation is the small sample size (n = 6). Research using donor
325 cadaveric tissue should be minimised to only what is essential and performed with
326 maximum efficiency and integrity out of respect for the donors. The characterisation
327 of cadaveric human tissue may not reflect the same response as living tissue.
328 However, ligamentous tissue primarily attributes its strength properties to the
329 collagen fibres which form the majority of ligament structure. The collagen would
330 not be greatly affected by the tissue being living or dead, providing it remains well
331 hydrated and is stored appropriately to abate tissue degradation. Although the
332 exclusion criteria required donors to have not reported any lower limb trauma we
333 cannot be certain that a prior sprain had not occurred at some point during the
334 donor's lifespan. It is estimated that ankle injury rates are approximately five and a
335 half times higher than those registered in emergency departments.¹³ This could
336 provide some explanation for the inconsistencies in strength between ligament types
337 (Figure 6). Large variations in the results following the mechanical characterisation of
338 ankle ligaments are also reported elsewhere.¹⁶ The use of elderly donor tissue to
339 investigate sprain has previously been suggested to be a limitation of cadaver
340 studies. An effort was therefore made when selecting donor specimens to obtain the
341 youngest specimens possible (mean 56.2 years). A previous study however, reported
342 no correlation between ultimate failure load and age for donors aged 17 to 54 when

343 testing human anterior cruciate ligaments.⁴ The link identified between BMI and
344 ultimate failure load of the CFL and PTFL is based on a narrow range of BMI with only
345 one donor having a BMI outside of the normal range and the trend may not be
346 reflected in a population at the extremities of the BMI scale.

347 **Conclusion**

348 Limitations aside, the conditions of this study were carefully defined to reflect those
349 experienced by individuals who would suffer an ankle sprain allowing for the entire
350 LCL complex to be characterised at realistic sprain inducing strain rates. In the
351 current study the ultimate failure load and stiffness of the ATFL, CFL and PTFL did not
352 differ systematically but there was a tendency toward greater strength in people
353 with a higher BMI. The maximum likely exposure loads, the BMI of the patient and
354 the failure mode of the LCLs all appear to be factors to be further considered when
355 selecting the material, repair or reconstruction technique to be used for surgical
356 stabilisation of the sprained ankle.

357 **Acknowledgements**

358 The authors would like to acknowledge Dr Nagitha Wijayathunga for his
359 contributions to the CT scanning of the samples.

360 **References**

- 361 1. Ajs A, Younger ASE, Maffulli N. Anatomic Repair for Chronic Lateral Ankle Instability.
362 *Foot Ankle Clin.* 2006;11(3):539-545. doi:10.1016/j.fcl.2006.07.005
- 363 2. de Asla RJ, Kozanek M, Wan L, Rubash HE, Li G. Function of anterior talofibular and
364 calcaneofibular ligaments during in-vivo motion of the ankle joint complex. *J Orthop*
365 *Surg Res.* 2009;4(1):7. doi:10.1186/1749-799X-4-7
- 366 3. Attarian DE, McCrackin HJ, DeVito DP, McElhaney JH, Garrett WE. Biomechanical
367 characteristics of human ankle ligaments. *Foot Ankle.* 1985;6(2):54-58.
368 doi:10.1177/107110078500600202
- 369 4. Blevins FT, Hecker AT, Bigler GT, Boland AL, Hayes WC. The Effects of Donor Age and
370 Strain Rate on the Biomechanical Properties of Bone-Patellar Tendon-Bone Allografts.
371 *Am J Sports Med.* 1994;22(3):328-333. doi:10.1177/036354659402200306
- 372 5. Bonnel F, Toullec E, Mabit C, Tourné Y. Chronic ankle instability: Biomechanics and
373 pathomechanics of ligaments injury and associated lesions. *Orthop Traumatol Surg*
374 *Res.* 2010;96(4):424-432. doi:10.1016/j.otsr.2010.04.003
- 375 6. Bonner TJ, Newell N, Karunaratne A, et al. Strain-rate sensitivity of the lateral
376 collateral ligament of the knee. *J Mech Behav Biomed Mater.* 2015;41:261-270.
377 doi:10.1016/j.jmbbm.2014.07.004
- 378 7. Colville MR, Marder RA, Boyle JJ, Zarins B. Strain measurement in lateral ankle
379 ligaments. *Am J Sports Med.* 1990;18(2):196-200. doi:10.1177/036354659001800214
- 380 8. Fong DT-P, Hong Y, Shima Y, Krosshaug T, Yung PS-H, Chan K-M. Biomechanics of
381 supination ankle sprain: a case report of an accidental injury event in the laboratory.
382 *Am J Sports Med.* 2009;37(4):822-827. doi:10.1177/0363546508328102
- 383 9. Funk JR, Hall GW, Crandall JR, Pilkey WD. Linear and Quasi-Linear Viscoelastic
384 Characterization of Ankle Ligaments. *J Biomech Eng.* 2000;122(1):15.
385 doi:10.1115/1.429623
- 386 10. Golanó P, Vega J, de Leeuw PAJ, et al. Anatomy of the ankle ligaments: a pictorial
387 essay. *Knee Surgery, Sport Traumatol Arthrosc.* 2016;24(4):944-956.
388 doi:10.1007/s00167-016-4059-4
- 389 11. Herbert A, Brown C, Rooney P, Kearney J, Ingham E, Fisher J. Bi-linear mechanical
390 property determination of acellular human patellar tendon grafts for use in anterior
391 cruciate ligament replacement. *J Biomech.* 2016;49(9):1607-1612.
392 doi:10.1016/j.jbiomech.2016.03.041
- 393 12. Hertel J. Functional anatomy, pathomechanics, and pathophysiology of lateral ankle
394 instability. *J Athl Train.* 2002;37(4):364-375. doi:10.1017/CBO9781107415324.004
- 395 13. Kemler E, van de Port I, Valkenberg H, Hoes AW, Backx FJG. Ankle injuries in the
396 Netherlands: Trends over 10-25 years. *Scand J Med Sci Sports.* 2015;25(3):331-337.
397 doi:10.1111/sms.12248
- 398 14. Quinn KP, Winkelstein BA. Preconditioning is correlated with altered collagen fiber
399 alignment in ligament. *J Biomech Eng.* 2011;133(6):575-579. doi:10.1115/1.4004205
- 400 15. Sarrafian SK. Anatomy of the Foot and Ankle. *JBLippincott Co.* 1983.
- 401 16. Siegler S, Schneck CD. The Mechanical Characteristics of the Collateral Ligaments of
402 the Human Ankle Joint. *Foot Ankle Int.* 1988;8(5):234-242.
403 doi:10.1177/107110078800800502
- 404 17. St Pierre RK, Rosen J, Whitesides TE, Szczukowski M, Fleming LL, Hutton WC. The
405 tensile strength of the anterior talofibular ligament. *Foot Ankle.* 1983;4(2):83-85.

406 doi:10.1177/107110078300400208

407 18. Stouffer DC, Butler DL, Hosny D. The relationship between crimp pattern and
408 mechanical response of human patellar tendon-bone units. *J Biomech Eng.*
409 1985;107(2):158-165. doi:10.1115/1.3138536

410